

External aerodynamics

- Chapter 4: drag components and control (part B) -

J. Boudet

Ecole Centrale de Lyon

November 20, 2020

Outline of chapter 4

Part A: boundary layers

- Boundary layer
- Transition
- Separation

Part B: drag components and control devices

- Drag contributions
- Boundary layer and drag control

Introduction: Breguet-Leduc equation (range)

[→ quiz]

Flight mechanics (chap. 1): level flight

$$T = D = L/f = W/f$$

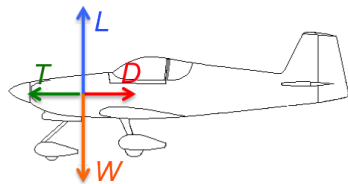
Specific fuel consumption: $C_s = Q/T$, where
 Q is the fuel mass flow (mass per unit of time).

Mass of fuel per distance unit:

$$\frac{C_s T}{V} = \frac{C_s W}{Vf}$$

When the aircraft covers a distance dR_a , its mass varies as:

$$dm = \frac{-C_s W}{Vf} dR_a$$



So the specific range is:

$$r_s = -\frac{dR_a}{dm} = \frac{Vf}{C_s W}$$

Consequently, the range is:

$$R = - \int_{m_1}^{m_2} r_s dm = - \int_{m_1}^{m_2} \frac{Vf}{C_s g m} dm = - \int_{m_1}^{m_2} \frac{LV}{DC_s g m} dm$$

→ varies with $1/D$.

Assuming f , V and C_s are constants:

$$R = \frac{Vf}{g C_s} \ln \left(\frac{m_1}{m_2} \right)$$

This shows the importance of drag minimization...

Contents

1. Drag contributions
 - Form drag
 - Skin friction drag
 - Induced drag
 - Interference drag
 - Trim drag
 - Cooling drag
 - Wave drag
2. Boundary layer and drag control
 - Influence of airfoil geometrical parameters
 - Delay transition
 - Counter separation
 - Winglets
3. Bibliography

Contents

1. Drag contributions

- Form drag
- Skin friction drag
- Induced drag
- Interference drag
- Trim drag
- Cooling drag
- Wave drag

2. Boundary layer and drag control

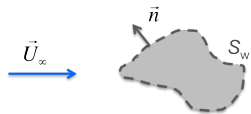
- Influence of airfoil geometrical parameters
- Delay transition
- Counter separation
- Winglets

3. Bibliography

Drag contributions

Fluid mechanics fundamentals [1]: expression of force on a body.

$$\underline{F} = \iint_{S_w} \underline{\sigma} \cdot \underline{n} dS$$



$$\text{where: } \underline{\sigma} = -P \underline{I} + \underline{\tau}$$

with: $\underline{\tau} = 2\mu \underline{\underline{S}} + \lambda(\nabla \cdot \underline{u}) \underline{I}$ for a Newtonian fluid (ex: air)

$$S_{ij} = \frac{1}{2} \left(\frac{\partial u_i}{\partial x_j} + \frac{\partial u_j}{\partial x_i} \right) \quad (\text{rate of strain})$$

Direct contribution of pressure (P) and friction ($\underline{\tau}$).

Drag contributions

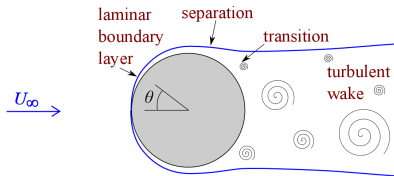
- Form drag (aka pressure drag)

Integral of the pressure force, projected in the flow direction.

$$D_{\text{press}} = - \iint_{S_w} P \underline{n} dS \cdot \underline{e}_{U_\infty} \quad \rightarrow \text{dominant contribution for bluff bodies.}$$

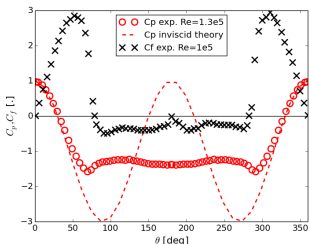
Example: circular cylinder in subcritical flow regime.

[→ quiz]

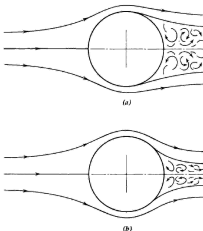


Separation at $C_f = 0 \Rightarrow$ lower pressure on the rear face of the cylinder \Rightarrow drag.
Note: drag scales with wake width.

$$C_p = \frac{P - P_\infty}{0.5 \rho_\infty U_\infty^2}$$

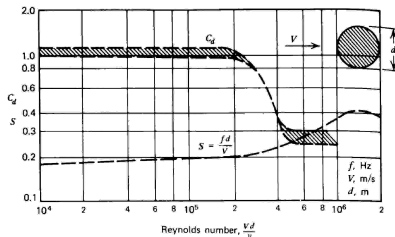


Influence of Re on the drag of a cylinder

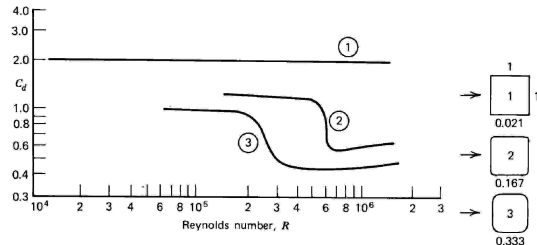


(a) low $Re \Rightarrow$
separation before
transition \Rightarrow thick
wake \Rightarrow large C_D .

(b) high $Re \Rightarrow$
transition before
separation \Rightarrow narrow
wake \Rightarrow low C_D .



Similar effect
with
round-cornered
square cylinders
→



Ratio 'corner radius' / 'side length' given below the sketches.

Drag contributions

- Skin friction drag

Integral of the viscous shear stresses,
projected in the flow direction:

$$D_{fric} = \iint_{S_w} \underline{\tau} \cdot \underline{e}_{U_\infty} \, dS$$

Exemple: horizontal tail of a Piper Cherokee (with
 $U_\infty = 60 \text{ m/s}$, $c = 0.762 \text{ m}$, $S_w = 4.65 \text{ m}^2$,
 $\rho = 1.054 \text{ kg.m}^{-3}$ and $\nu = 1.639 \cdot 10^{-5} \text{ m}^2/\text{s}$).



Estimate using flat plate correlations (note: ∇P is neglected):

$$Re_T = 3 \cdot 10^5 \Rightarrow x_T = 0.082 \text{ m}$$

$$D_{fric}^{(lam)} = \left(\int_0^{0.082} 0.664 \left(\frac{U_\infty x}{\nu} \right)^{-1/2} dx \right) \times \frac{S_w}{c} \times \frac{1}{2} \rho U_\infty^2 = 2.30 \text{ N}$$

$$D_{fric}^{(turb)} = \left(\int_{0.082}^{0.762} 0.0368 \left(\frac{U_\infty x}{\nu} \right)^{-1/6} dx \right) \times \frac{S_w}{c} \times \frac{1}{2} \rho U_\infty^2 = 27.71 \text{ N}$$

[\[→ quiz\]](#)

Fluid mechanics fundamentals:

$$\text{Form drag} + \text{Skin friction drag} = \text{Total drag}$$

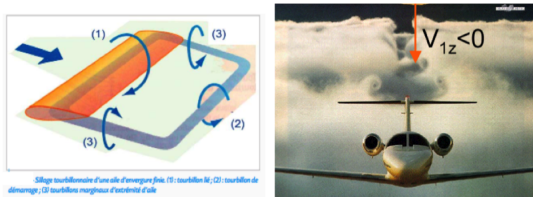
$$D_{\text{press}} + D_{\text{fric}} = D$$

However, in practical aerodynamics, specific contributions to drag are identified [2], in relation to design parameters. Those contributions affect D_{press} and D_{fric} . The major ones are listed below.

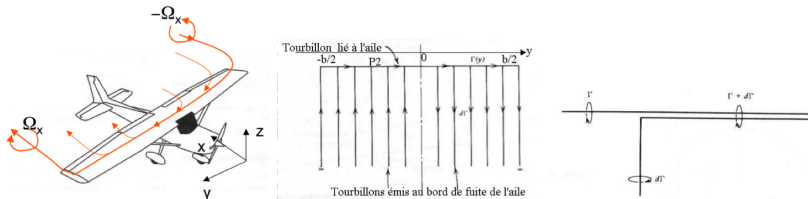
Drag contributions

- Induced drag

From chapter 3: lift on a finite span wing (3D) is source of axial vorticity.



Lifting surface and lifting line methods:



According to lifting surface theory, the induced drag writes:

$$D_i = \frac{\rho}{4\pi} \int_{-b/2}^{b/2} \int_{-b/2}^{b/2} \Gamma(y) \frac{d\Gamma}{dy'} \frac{dy' dy}{y - y'}$$

It is minimum for an elliptic loading distribution $\Gamma(y)$:

$$C_{Di} = \frac{C_L^2}{\pi A} \quad \text{with: } A = \frac{b^2}{S}$$

For other loading distributions, this expression can be generalised with *Oswald's efficiency factor* $e < 1$:

$$C_{Di} = \frac{C_L^2}{\pi A} (1 + \delta) = \frac{C_L^2}{\pi Ae}$$

According to lifting line theory ($A \gg 1$), each wing section is equivalent to a 2D profile with the effective angle of attack:

$$\alpha_e = \alpha + \epsilon(y) + \alpha_i(y) \quad \text{where } \epsilon(y) \text{ is the twist angle and:}$$

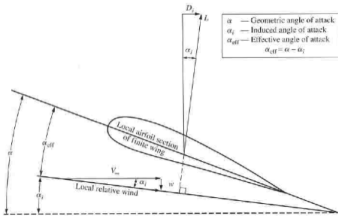
$$\alpha_i(y) = \frac{1}{4\pi V_\infty} \int_{-b/2}^{b/2} \frac{d\Gamma}{dy'} \frac{dy'}{y' - y} < 0$$

And for an elliptic loading:

$$\alpha_i = \frac{-C_L}{\pi A}$$

$$C_L = C_{L\alpha} \left(\alpha - \alpha_0^{\text{wing}} \right) \quad \text{with: } \alpha_0^{\text{wing}} = \alpha_0 - \epsilon$$

$$C_{L\alpha} = \frac{2\pi}{1 + 2/A}$$



The induced drag, related to the generation of lift, is generally distinguished from the other sources of drag, gathered within the *parasite drag* (form drag, friction drag...).

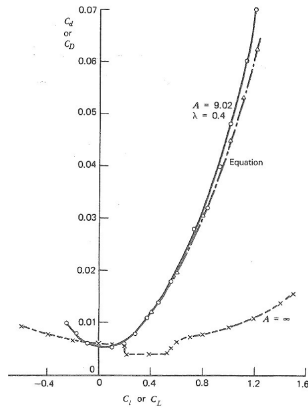
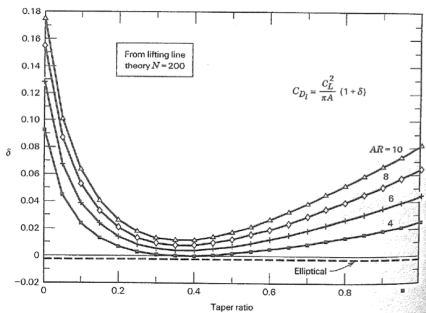
Parasite and induced drag decomposition on a linearly tapered wing

$$c(y) = c_0 [1 - (1 - \lambda)|2y/b|]$$

$\lambda = c(y = b/2)/c(y = 0)$: taper ratio

$A = AR = b^2/S$: aspect ratio

lifting line theory $\rightarrow (1 + \delta) = 1/e$



$$C_D = C_{Dmin} + k C_L^2 + \frac{C_L^2}{\pi A e} = C_{Dmin} + \frac{C_L^2}{\pi A e'}$$

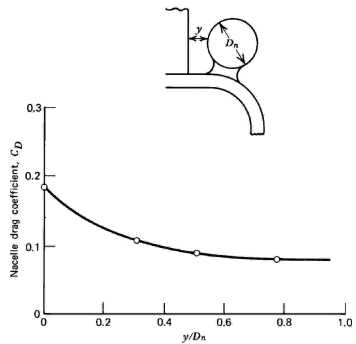
C_{Dmin} and k : measured on the profile ($A = +\infty$), e : from lifting line.
In the figure: $e' = 0.89$.

Drag contributions

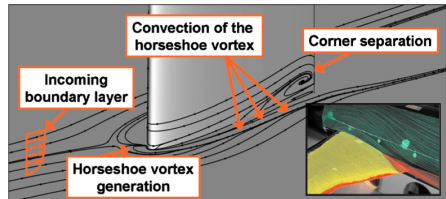
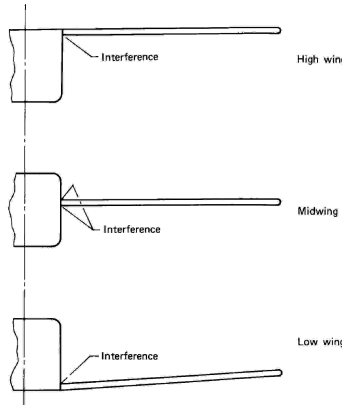
- Interference drag

The drag of two nearby elements can be superior to the sum of drags of the isolated elements.

Example: engine nacelle / rotor pylon
on a tandem helicopter (CH-47).



Another example: wing-fuselage interference.



source: Tinoco, 3rd CFD drag prediction workshop, 2006

Low wing configurations:

- Possible *corner separation* because fuselage BL and suction-side BL interact \Rightarrow drag increase.
[→ quiz]
- But: increased ground effect during take-off and landing.

Interference can be also favorable (i.e. interference drag < 0): e.g. drafting or slipstreaming.

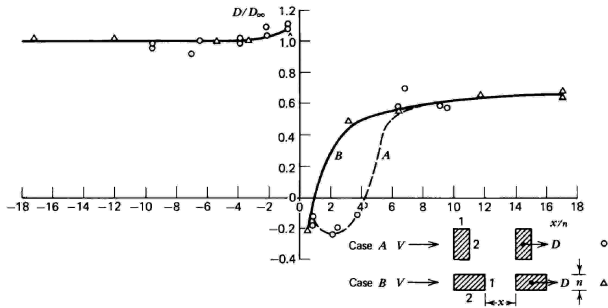


Figure: Evolution of drag of an object depending on its position in a tandem.

Significant reduction of drag when downstream.

Drag contributions

- Trim drag

What is the influence of the plane equilibrium (wing / horizontal stabilizer) on drag, given that C_{Di} varies with C_L^2 ?

Modification of wing drag by transfer of lift to the stabilizer:

$$L_w + L_t = \text{weight} \Rightarrow C_{Lw} + \frac{S_t}{S_w} C_{Lt} = C_L$$

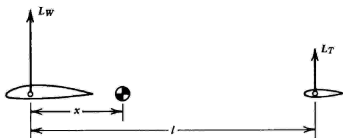
Drag on stabilizer:

$$C_{Dit} = \frac{C_{Lt}^2}{\pi A_t e_t} \frac{S_t}{S_w} = \frac{S_t}{S_w} C_{Di} \frac{C_{Lt}^2}{C_L^2} \frac{A_w e_w}{A_t e_t}$$

$$\begin{aligned} C_{Diw} &= \frac{C_{Lw}^2}{\pi A_w e_w} \approx \frac{C_L^2}{\pi A_w e_w} - 2 \frac{S_t}{S_w} \frac{C_{Lt} C_L}{\pi A_w e_w} \\ &\approx \underbrace{\frac{C_L^2}{\pi A_w e_w}}_{C_{Di}} - \underbrace{2 C_{Di} \frac{C_{Lt} S_t}{C_L S_w}}_{\Delta C_{Diw}} \end{aligned}$$

indices: w: wing, t: tail

Coefficients: S_w used as common normalization area.



Center of gravity positioning:

$$xL_w = (l - x)L_t, \quad L_w + L_t = \text{weight}$$

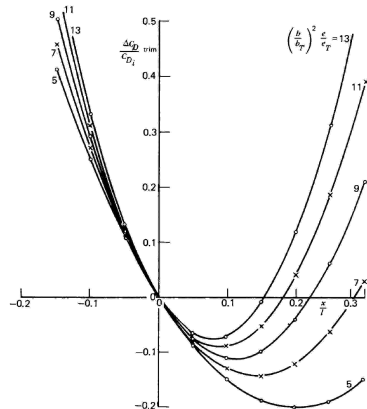
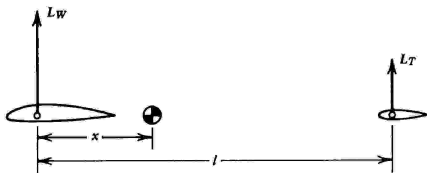
$$\Rightarrow L_t = \frac{x}{l} \text{ weight} \Rightarrow \frac{S_t}{S_w} \frac{C_{Lt}}{C_L} = \frac{x}{l}$$

$$\Delta C_{Dtrim} = \Delta C_{Diw} + C_{Dit}$$

$$\frac{\Delta C_{Dtrim}}{C_{Di}} = \frac{x}{l} \left(\frac{x}{l} \left(\frac{b_w}{b_t} \right)^2 \frac{e_w}{e_t} - 2 \right)$$

Orders of magnitude:

$$e_w \approx e_t, \quad b_w \approx 3b_t$$



[→ quiz]

Chapter 1: move centre of gravity forward of neutral point for *static stability* in pitch \Rightarrow possible $L_t < 0 \Rightarrow$ drag increase.

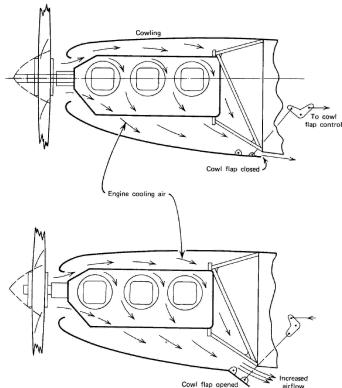
Drag contributions

- Cooling drag

Air withdrawal for cooling, ventilation...

Momentum budget: $D_{ventil} \approx \dot{m}(V_{in} - V_{out})$

where: \dot{m} : mass flow, V_{in} & V_{out} : inflow & outflow velocities.



Neglecting the temperature variation in the total enthalpy budget:

$$Q + W_{ventil} \approx \frac{1}{2} \dot{m} (V_{in}^2 - V_{out}^2)$$

$$\approx D_{ventil} \frac{V_{in} + V_{out}}{2}$$

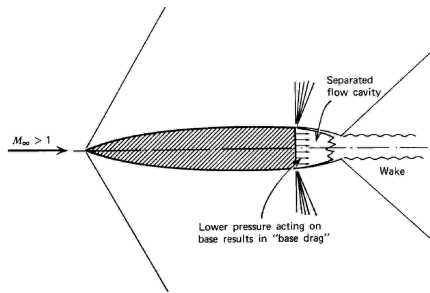
Air withdrawal in turbojet engines \Rightarrow reduction of thrust.

Drag contributions

- Wave drag

Additional drag component in transonic and supersonic regimes, involving shocks (\Rightarrow entropy) and expansion waves.

Example: supersonic bullet.



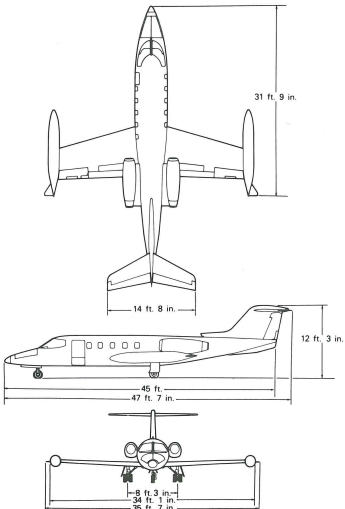
Developed in chapter 5.

Drag contributions

- Drag breakdown example

Gates Learjet Model 25 (source:
McCormick [2])

Item	C_d (based on wing planform area)	Percent of total
Wing	0.0053	23.45
Fuselage	0.0063	27.88
Tip tanks	0.0021	9.29
Tip tank fins	0.0001	0.44
Nacelles	0.0012	5.31
Pylons	0.0003	1.33
Horizontal tail	0.0016	7.08
Vertical tail	0.0011	4.86
Interference	0.0031	13.72
Roughness and gap	0.0015	6.64
Total	0.0226	100.00



Contents

1. Drag contributions

- Form drag
- Skin friction drag
- Induced drag
- Interference drag
- Trim drag
- Cooling drag
- Wave drag

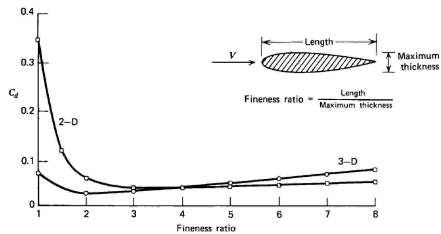
2. Boundary layer and drag control

- Influence of airfoil geometrical parameters
- Delay transition
- Counter separation
- Winglets

3. Bibliography

Boundary layer and drag control

- Influence of airfoil geometrical parameters



→ benefit of streamlined shapes.

Low aspect ratio: form drag favored.
High aspect ratio: skin friction drag favored.

Figure: Evolution of C_D with fineness ratio.
3D: axi-symmetric shape. $Re \approx 10^7$ based on length. C_D based on frontal area.

NACA airfoils:

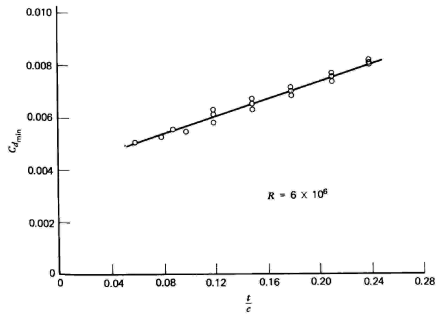


Figure: Minimum drag coefficient, for NACA 4- and 5-digit airfoils. C_d based on chord length. For a given fineness ratio ($t/c = \text{thickness} / \text{chord length}$), the different points represent different values of camber.

[→ quiz]

- Little influence of camber.
- Nearly linear evolution against t/c .
- For $t/c = 0$, a flat plate estimate of friction drag yields $C_d \approx 0.0042$ for $Re_T = 2.4 \cdot 10^6$.

Boundary layer and drag control

- Delay transition

Motivation: reduced friction in laminar regime.

Hypotheses for illustration:

- 2D, incompressible
- $\mu(T)$, with wall cooling or heating: $T(y)$
- wall: $u = 0$, with suction or blowing: $v = V_w$

x -momentum equation at wall ($y = 0$):

$$\underbrace{\rho \frac{\partial u}{\partial t} + \rho u \frac{\partial u}{\partial x}}_{=0} + \underbrace{\rho v \frac{\partial u}{\partial y}}_{=0} = -\frac{\partial P}{\partial x} + \frac{\partial}{\partial x} \left(2\mu \underbrace{\frac{\partial u}{\partial x}}_{=0} \right) + \frac{\partial}{\partial y} \left(\mu \frac{\partial u}{\partial y} + \mu \underbrace{\frac{\partial v}{\partial x}}_{=0} \right)$$

$$\left(\rho V_w - \frac{\partial \mu}{\partial T} \frac{\partial T}{\partial y} \right) \frac{\partial u}{\partial y} + \frac{\partial P}{\partial x} = \mu_w \frac{\partial^2 u}{\partial y^2}$$

$$\text{At wall } (y=0): \quad \left(\rho V_w - \frac{\partial \mu}{\partial T} \frac{\partial T}{\partial y} \right) \frac{\partial u}{\partial y} + \frac{\partial P}{\partial x} = \mu_w \frac{\partial^2 u}{\partial y^2}$$

Note:

$$\int_0^\delta \frac{\partial^2 u}{\partial y^2} dy = \frac{-\tau_w}{\mu}$$

Attached boundary layer: $\tau_w > 0$ and $\partial^2 u / \partial y^2(y = 0) < 0$.

Cf. chap.4 part A: stabilization of the boundary layer when momentum increases near wall or wall friction ↗

⇒ promote $\partial^2 u / \partial y^2(y = 0) < 0$, through:

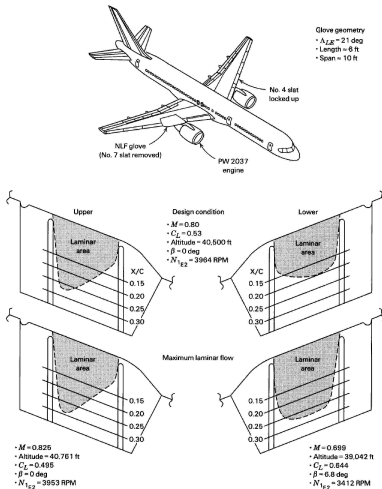
[→ quiz]

- Favorable pressure gradient ($\partial P / \partial x < 0$).
- Suction at wall ($V_w < 0$), reducing also the BL thickness.
- Wall cooling ($\partial \mu_{air} / \partial T > 0$, $\partial T / \partial y > 0$).

+ control of roughness, limitation of inflow turbulence...

Influence of Re and C_L must be kept in mind.

Natural laminar flow (NLF): passive techniques.



Laminar flow control (LFC): active techniques.

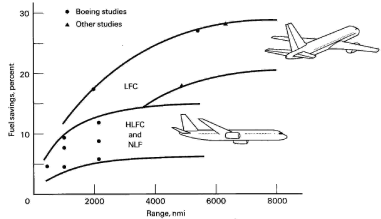


Figure 4.50 Predicted fuel savings for subsonic transports from the application of laminar flow control.

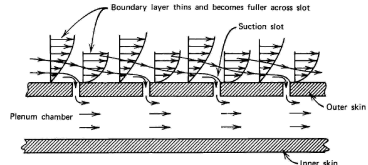
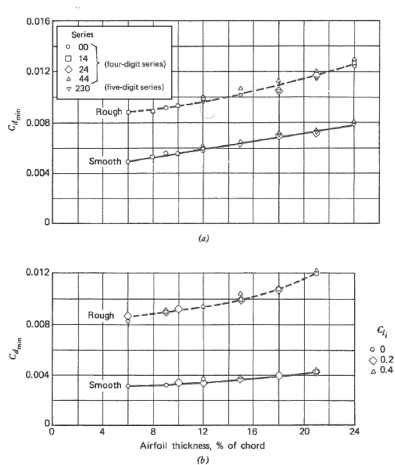
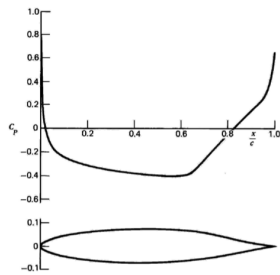


Figure 4.48 Laminar flow control (LFC) by suction through thin slots transverse to the flow.

Airfoil shape (NLF): NACA 66 series example.
Laminar BL extended by favorable $\partial P/\partial x$.



(a): NACA 4/5 digits, (b): NACA 66 series.



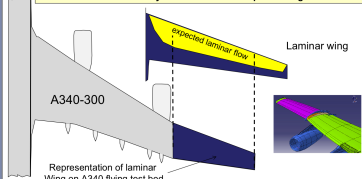
Chordwise pressure distribution for the NACA 66₀₁₅ airfoil.

On-going NLF study in EU research project *Clean Sky - SFWA*.

Flight tests: cf. *Air & Cosmos*, Sept. 2017.

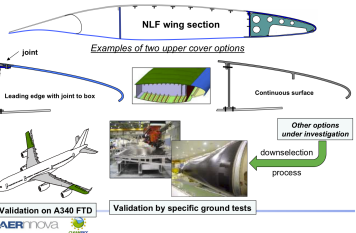
Aeronautics priority R&T in CleanSky

Major Objective:
Demonstrate the feasibility of a structure concept enabling laminar flow



AERmova


Laminar Wing Structure Options & Validation



Examples of LFC studies:



NASA (1963): Northrop X-21 with
~ 800 000 suction holes.
⇒ laminar BL over 95% of wing
surface, but arduous maintenance...



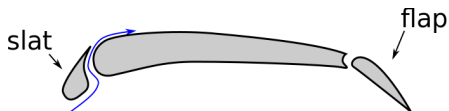
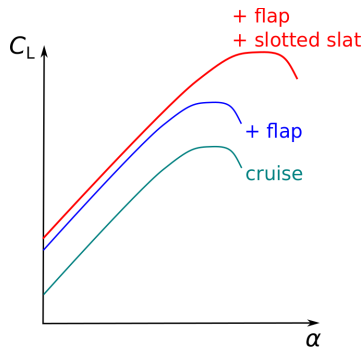
NASA Dryden (1988-1996): F-16XL
with porous titanium element on left
wing and suction device
⇒ laminar BL over 46% of the
element, for $M = 0.2$.

Boundary layer and drag control

- Counter separation

- High-lift devices:

Increase C_L during take-off or landing (reduced speed).



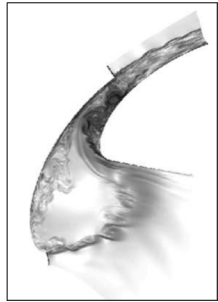
Principle: increase camber and surface. Moreover, slots act again separation by energizing the BL: air is driven from pressure side to suction side ($\Delta P < 0$), accelerated ($\Delta S < 0$) and reinjected tangentially to the wall.



Slat and flaps on an Airbus 300.



Slotted flaps on a Boeing 747 (photograph by Adrian Pingstone, public domain).



Schlieren visualization of LES simulation in a slat channel (Terracol, 2005).

Drawbacks of high-lift devices:

- drag increase \Rightarrow retracted during cruise;
- noise sources (airframe noise).

- Vortex generators:



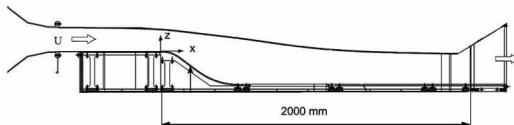
VG on nacelles. Vortices are revealed by condensation.



VG on a Douglas A4 wing.

Principle: generate streamwise vorticity in order to transfer momentum to sensitive flow regions (boundary layer...).

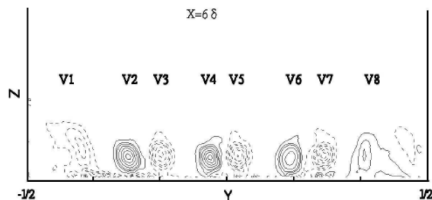
Experimental study of Gardarin *et al.* [3]: control of flow separation with VG, in a divergent flow channel.



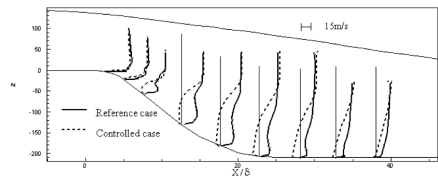
Wind tunnel.



VG layout (view from above).



Vorticity contours in a cross-section downstream of the VG. Dashed lines: negative values.



Velocity profiles in the wind tunnel.

→ VG reduce flow separation (controlled case, error in figure?).

Boundary layer and drag control

- Winglets

Mechanism: lift component directed forward.

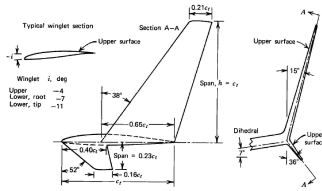
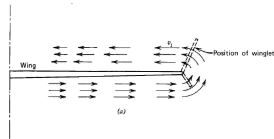
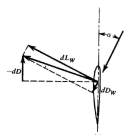


Figure 4.32 Winglet geometry.

$$\Delta D = -L_{wgt} \alpha_{wgt} + D_{wgt}$$

$$\Delta C_D \approx \frac{-S_{wgt}}{S} \left(C_{Lwgt} \alpha_{wgt} - C_{D0wgt} - \frac{C_{Lwgt}^2}{\pi A_{wgt}} \right)$$

Objective: $\Delta C_D < 0$



$$\text{Model: } \alpha_{wgt} = K C_L \text{ and: } C_{Lwgt} = \frac{2\pi}{1 + 2/A_{wgt}} \alpha_{wgt}$$

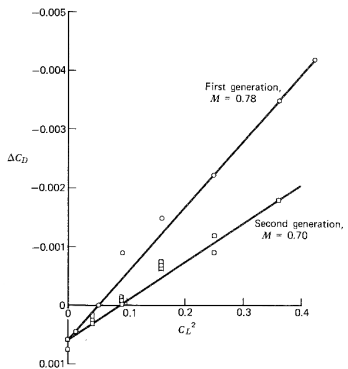
$$\Delta C_D \approx \frac{-S_{wgt}}{S} \left(\frac{2\pi}{1 + 2/A_{wgt}} \left(1 - \frac{2/A_{wgt}}{1 + 2/A_{wgt}} \right) K^2 C_L^2 - C_{D0wgt} \right)$$

$$\Delta C_D \approx \frac{-S_{wgt}}{S} \left(\frac{2\pi K^2 C_L^2}{(1 + 2/A_{wgt})^2} - C_{D0wgt} \right)$$

Benefit increases with: S_{wgt}/S , C_L^2 and A_{wgt} .



A320neo "sharklet". Span (=height): 2.4 m.
 $\Delta C_D \sim -4\%$. Source: Airbus.



Influence of winglets on 1st and 2nd generation aircrafts (for example, DC-10 is 2nd generation). Observe $\Delta C_D \sim C_L^2$.

Glossary

English

aspect ratio (A)

camber

drag

flap

high-lift device

lift

slat

taper ratio (λ)

thickness

wake

French

allongement

cambrure

traînée

volet

dispositif hypersustentateur

portance

bec

effilement

épaisseur

sillage

Bibliography

- [1] J. Scott, M. Gorokhovski, C. Corre, and C. Bailly, *Fluides et énergie*. Ecole Centrale de Lyon, 2017.
- [2] B. W. McCormick, *Aerodynamics, Aeronautics and Flight Mechanics*. John Wiley and Sons, 1995.
- [3] B. Gardarin, L. Jacquin, and P. Geffroy, "Flow Separation Control With Vortex Generators," in *4th Flow Control Conference*. Seattle: AIAA, Jun. 2008, pp. AIAA 2008-3773.